Chemistry–A European Journal

Supporting Information

The Butterfly Complex [{Cp*Cr(CO)$_3$}$_2$(μ,$\eta^{1:1}$-P$_4$)] as a Versatile Ligand and Its Unexpected P$_1$/P$_3$ Fragmentation

Rebecca Grünbauer, Gábor Balázs, and Manfred Scheer*[a]

SUPPORTING INFORMATION

Table of Contents

SUPPORTING INFORMATION

Experimental Procedures

All experiments were carried out under an atmosphere of dry argon or nitrogen using glovebox and schlenk techniques. Residues of oxygen and water were removed from the inert gas by passing it over a BASF R 3-11 ($CuO/MgSiO_3$) catalyst, concentrated H_2SO_4 and finally granulated silica gel. Dry solvents were collected from a Braun SPS Apparatus and degassed prior to use. The deuterated solvents C_6D_6 and CD_2Cl_2 were degassed and dried by stirring with Na/K alloy and CaH_2, respectively, followed by distillation. After the distillation, CD_2Cl_2 was additionally stored over molecular sieve (3 Å) which had previously been dried for four hours under high vacuum at 100 °C. [{Cp*Cr(CO)$_3$}$_2$(μ,η$^{1:1}$-P_4)] (**1**)[1] and [M(CO)$_4$(nbd)] (M = Cr, Mo, W)[2] were prepared according to literature procedures.

NMR spectra were recorded at the NMR department of the University Regensburg using a Bruker Advance 300 or 400 spectrometer. Samples are referenced against TMS (^{1}H, ^{13}C) or 85% H_3PO_4 (^{31}P) as external standards. Chemical shifts (δ) are reported in ppm and coupling constants (*J*) in Hz. The spectra were processed using the TopSpin 3.0 software (Bruker) and the WIN-DAISY module of this software was used to perform simulations.[3]

FD and LIFDI-MS spectra were measured by the MS department of the University Regensburg on an AccuToF GCX (Jeol) spectrometer. The observed fragments were assigned according to the mass/charge (m/z) ratio and the isotope pattern.
IR spectra were recorded on an ALPHA platinum ATR spectrometer (Bruker Optik GmbH) which was placed inside a glove box. Therefore, the air-sensitive solid samples could be placed directly on the spectrometer without any additional preparative measures.
Elemental analyses were performed by the department of central analyses of the University Regensburg on a Vario micro cube instrument (Elementar Analysensysteme GmbH).

Crystallographic measurements were performed on a GV50 diffractometer with a Titan S2 detector (**2**, **3-1a** and **4**), an Oxford Diffraction Supernova diffractometer with an Atlas CCD detector (**3-2a)** or an Oxford Diffraction Gemini Ultra (**3-2b**) with an Atlas S2 detector operating at T = 123.01(13) K.[4] An analytical absorption correction was carried out for all measurement using the CrysAlisPro software.[5] The structure solution and refinement was performed using the ShelXT and ShelXL module of the Olex2 (version 1.2.7) software.[6] Hydrogen atoms were modeled in idealized positions and refined isotropically.

DFT calculations were performed by Dr. Gábor Balázs (University Regensburg) with the TURBOMOLE[7] program package at the (RI-)[8]BP86[9]/def2-TZVP[6b,10] level of theory. The Multipole Accelerated Resolution of Identity (MARI-J)[11] approach was used to speed up the geometry optimizations which were performed without any symmetry restrains. The total energies were calculated by single point calculations without using the RI formalism. The SCF energies were used without corrections and the entropic effects are not considered.

Synthesis of [{Cp*Cr(CO)$_3$}$_2$(μ$_3$,η$^{1:1:1:1}$-P_4){W(CO)$_4$}] (2)

A dark orange solution of **1** (100 mg, 0.15 mmol, 1.0 eq.) in thf (5 mL) is added to a slightly yellow solution of [W(CO)$_4$(nbd)] (59 mg, 0.15 mmol, 1.0 eq.) in thf (5 mL). The resulting mixture is stirred at room temperature for 3 days. Hereby, the color of the solution changes from dark orange to red. The solvent is subsequently removed under reduced pressure. The resulting red solid is washed with *n*-hexane and dried in vacuo. To obtain pure **2**, *n*-pentane (15 mL) is slowly added to a concentrated solution of the crude product in dichloromethane (2 mL). Hereby, **2** precipitates as a dark red powder. Crystals suitable for single crystal X-ray analysis were obtained from a saturated solution in *n*-hexane (5 mL) and dichloromethane (1 mL) after storage at -28 °C.

Analytical data for 2

Yield	70 mg (0.8 mmol, 48%)
^{1}H NMR (C_6D_6)	δ[ppm] = 1.42 (s, 30H, $C_5(C\underline{H}_3)_3$)
^{31}P NMR (C_6D_6)	δ[ppm] = -153.8 (m, 2P, P_A), -168.8 (m, 2P, P_B)
^{31}P{^{1}H} NMR (C_6D_6)	δ[ppm] = -153.8 (m, 2P, P_A), -168.8 (m, 2P, P_B)
IR (solid)	$\tilde{\nu}_{CO}$ [cm^{-1}] = 2069 (s), 2019 (s, br), 2006 (s, br), 1992 (s, br), 1988 (s, br)
ES-MS (toluene)	No reasonable peaks detectable.
LIFDI-MS (toluene)	No reasonable peaks detectable.

Synthesis of [{Cp*Cr(CO)$_2$}$_2$(μ$_3$,η$^{3:1:1}$-P_4){Cr(CO)$_5$}] (3a)

A dark orange solution of **1** (100 mg, 0.15 mmol, 1.0 eq.) in thf (5 mL) is added to a yellow solution of [Cr(CO)$_4$(nbd)] (39 mg, 0.15 mmol, 1.0 eq.) in thf (5 mL). The resulting mixture displays a color change from orange to red while it is stirred at room temperature for 3 d. Subsequently, the solvent is removed under reduced pressure. The resulting solid is dried in vacuo and dissolved in CH_2Cl_2 (10 mL). Upon storage at -78°C for two weeks and subsequent storage at -28°C for three months, a few single crystals of **3a** can be obtained.

Analytical data for (3a)

^{31}P{^{1}H} NMR (CD_2Cl_2)	δ[ppm] = 22.3 (dd, $^1J_{MX}$ = 306 Hz, $^1J_{NX}$ = 290 Hz, 1P, P_X), 166.3 (dd, $^1J_{AN}$ = 257 Hz, $^1J_{NX}$ = 290 Hz, 1P, P_N), 226.3 (dd, $^1J_{AM}$ = 251 Hz, $^1J_{MX}$ = 306 Hz, 1P, P_M), 515.4 ppm (m, 1P, P_A)

Synthesis of [{Cp*Cr(CO)$_2$}$_2$(μ$_4$,η$^{3:1:1:1}$-P_4){Cr(CO)$_5$}$_2$] (4a)

A dark orange solution of **1** (200 mg, 0.3 mmol, 1.0 eq.) in thf (5 mL) is added to a yellow solution of [Cr(CO)$_4$(nbd)] (154 mg, 0.6 mmol, 2.0 eq.) in thf (5 mL). The resulting mixture is stirred at room temperature for 20 h. Hereby, the color of the solution darkens. The solvent is removed under reduced pressure yielding a brown-purple solid that is washed with *n*-pentane. The solid is taken up in dichloromethane (2 mL) and upon storage at -28°C pure **4a** is obtained in the form of purple crystals that are suitable for single crystal X-ray analysis.

SUPPORTING INFORMATION

Analytical data for 4a

Yield	184 mg (0.18 mmol, 60%)
^{1}H NMR (CD_2Cl_2)	δ[ppm] = 1.84 (s, 15H, $C_5(C\underline{H}_3)_3$), 2.15 (s, 15H, $C_5(C\underline{H}_3)_3$)
^{13}C{^{1}H} NMR (CD_2Cl_2)	δ[ppm] = 11.4 (s, $C_5(\underline{C}H_3)_3$), 12.0 (s, $C_5(\underline{C}H_3)_3$), 103.3 (s, $\underline{C}_5(CH_3)_3$), 105.8 (s, $\underline{C}_5(CH_3)_3$), 212.2 (s, CO), 214.7 (s, CO), 215.9 -216.1 (m, CO), 221.2 (s, CO), 221.9 (s, CO)
^{31}P{^{1}H} NMR (CD_2Cl_2)	δ[ppm] = 107.9 (ddd, $^{2}J_{AX}$ = 28 Hz, $^{1}J_{MX}$ = 300 Hz, $^{1}J_{NX}$ = 330 Hz, 1P, P_X), 150.5 (ddd, $^{2}J_{MN}$ = 19.5 Hz, $^{1}J_{AN}$ = 252 Hz, $^{1}J_{NX}$ = 330 Hz, 1P, P_N), 219.5 (ddd, $^{2}J_{MN}$ = 19.5 Hz, $^{1}J_{AM}$ = 254 Hz, $^{1}J_{MX}$ = 300 Hz, 1P, P_M), 489.1 ppm (dt, $^{2}J_{AX}$ = 28 Hz, $^{1}J_{AM}$ resp. $^{1}J_{AN}$ = 254 Hz, 1P, P_A)
IR (solid)	$\tilde{\nu}_{CO}$ [cm^{-1}] = 2069 (s), 2055 (s), 1995 (s), 1977 (m), 1921 (s, br), 1909 (s,br), 1867 (s, br)
LIFDI-MS (toluene)	m/z [%] = 993.85 $[M]^+$ (100), 801.92 $[M\text{-}Cr(CO)_5]^+$ (10)
Elemental Analysis	calcd. for $C_{34}H_{30}Cr_4O_{14}P_4\cdot(CH_2Cl_2)$ (1079.42 g mol^{-1}) C 38.95, H 2.99; found C 39.09, H 3.07.

Synthesis of [{Cp*Cr(CO)$_2$}$_2$(μ$_4$,η$^{3:1:1:1}$-P$_4$){Mo(CO)$_5$}$_2$] (4b)

A dark orange solution of **1** (100 mg, 0.15 mmol, 1.0 eq.) in thf (5 mL) is added to a yellow solution of $[Mo(CO)_4(nbd)]$ (90 mg, 0.30 mmol, 2.0 eq.) in thf (5 mL). The resulting mixture is stirred at room temperature for 20 h while the color of the solution turns from orange to dark brown. The solvent is removed under reduced pressure yielding a brown solid that is washed with *n*-pentane. The solid is subsequently taken up in a mixture of dichloromethane (2 mL) and *n*-pentane (5 mL). Upon storage at -28°C pure **4b** is obtained in the form of black crystals that are suitable for single crystal X-ray analysis.

Analytical data for 4b

Yield	83 mg (0.76 mmol, 51 %)
^{1}H NMR (CD_2Cl_2)	δ[ppm] = 1.84 (s, 15H, $C_5(C\underline{H}_3)_3$), 2.14 (s, 15H, $C_5(C\underline{H}_3)_3$)
^{13}C{^{1}H} NMR (CD_2Cl_2)	δ[ppm] = 11.4 (s, $C_5(\underline{C}H_3)_3$), 12.0 (s, $C_5(\underline{C}H_3)_3$), 103.2 (s, $\underline{C}_5(CH_3)_3$), 105.4 (s, $\underline{C}_5(CH_3)_3$) (no signals for CO ligands detectable)
^{31}P{^{1}H} NMR (CD_2Cl_2)	δ[ppm] = 75.2 (m, 1P, P_X), 152.9 (m, 1P, P_N), 192.2 (m, 1P, P_M), 487.8 ppm (td, $^{2}J_{AX}$ = 24 Hz, $^{1}J_{AM}$ resp. $^{1}J_{AN}$ = 248 Hz, 1P, P_A)
IR (solid)	$\tilde{\nu}_{CO}$ [cm^{-1}] = 2078 (m), 2067 (m), 1997 (m, br), 1979 (m, br), 1924 (s, br), 1909 (s,br), 1865 (s, br)
LIFDI-MS (toluene)	m/z [%] = 1081.77 $[M]^+$ (100), 847.85 $[M\text{-}Mo(CO)_5]^+$ (24)

Fragmentation of [{Cp*Cr(CO)$_2$}$_2$(μ$_4$,η$^{3:1:1:1}$-P$_4$){Cr(CO)$_5$}$_2$] (4a) and in situ reactivity of [{Cp*Cr(CO)$_2$}(μ$_3$-P){Cr(CO)$_5$}$_2$] (6) affording [{Cp*Cr(^{t}Bu-NC)(CO)$_2$}(μ$_3$-P){Cr(CO)$_5$}$_2$] (7)

A brown solution of **4a** (20 mg, 0.02 mmol, 1.0 eq.) in thf (50 mL) is stirred at 50 °C for 3 d. Using $^{31}P\{^{1}H\}$ NMR spectroscopy, the consumption of the starting material can be monitored an two new signals are obtained. ^{t}Bu-NC (1 mL, 8.8 mmol, 440 eq.) is added to the reaction solution and no color change can be observed. Again, with the help of $^{31}P\{^{1}H\}$ NMR spectroscopy the immediate quantitative reaction of **6** to **7** is observed, while the signal for **5** stays unchanged.

Analytical data

^{31}P{^{1}H} NMR (**5**,thf with C_6D_6-capillary)	δ[ppm] = -273.3 (s, 3P)
^{31}P{^{1}H} NMR (**6**,thf with C_6D_6-capillary)	δ[ppm] = 1123.7 (s, 1P)
^{31}P{^{1}H} NMR (**7**,thf with C_6D_6-capillary)	δ[ppm] = -166.4 (s, 1P)

Results and Discussion

1. NMR experiments

[{Cp*Cr(CO)$_3$}$_2$(μ$_3$,η$^{1:1:1:1}$-P$_4$){W(CO)$_4$}] (2)

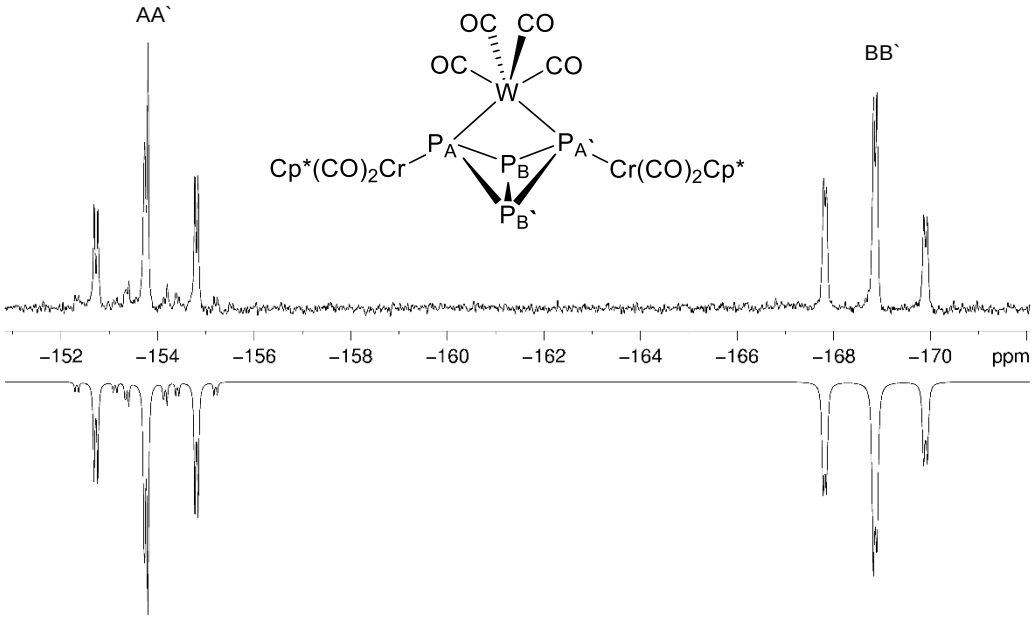

Figure S1. Experimental (top) and simulated (bottom) $^{31}P\{^1H\}$ NMR spectrum of **2** in C_6D_6.

Table S1. Experimental and simulated values for the chemical shifts and coupling constants in the $^{31}P\{^1H\}$ NMR spectrum of **2**.

	Exp.	F1 (85.69%)	F2 (14.28%)		Exp.	F1 (85.69%)	F2 (14.28%)
δ_A	-153.8 ppm	-153.8 ppm	-153.8 ppm	$^1J_{AB}$	168 Hz	169.2 Hz	169.4 Hz
				$^1J_{AB`}$	168 Hz	169.2 Hz	168.7 Hz
$\delta_{A`}$	-153.8 ppm	-153.8 ppm	-153.8 ppm	$^1J_{A`B}$	168 Hz	169.2 Hz	169.4 Hz
				$^1J_{A`B`}$	168 Hz	169.2 Hz	168.7 Hz
δ_B	-168.8 ppm	-168.8 ppm	-168.8 ppm	$^2J_{AA`}$	11 Hz	35.0 Hz	35.0 Hz
				$^2J_{BB`}$	11 Hz	15.4 Hz	18.7 Hz
$\delta_{B`}$	-168.8 ppm	-168.8 ppm	-168.8 ppm	$^1J_{AW}$	-	-	128.3 Hz
				$^1J_{A`W}$	-	-	129.0 Hz
				$^2J_{BW}$	-	-	9.8 Hz
				$^2J_{B`W}$	-	-	9.8 Hz

The simulation of the $^{31}P\{^1H\}$ NMR spectrum of **2** was carried out on the basis of an AA`BB` spin system with a C_1 symmetry. According to the natural abundancy of the NMR active ^{138}W isotope, the simulation was performed using two fragments. The main fragment (F1, 85.69%) was simulated with an NMR inactive tungsten atom, whereas the second fragment (F2, 14.28%) considered the ^{138}W atom.

[{Cp*Cr(CO)$_2$}$_2$(μ$_3$,η$^{3:1:1}$-P$_4$){Cr(CO)$_5$}] (3a)

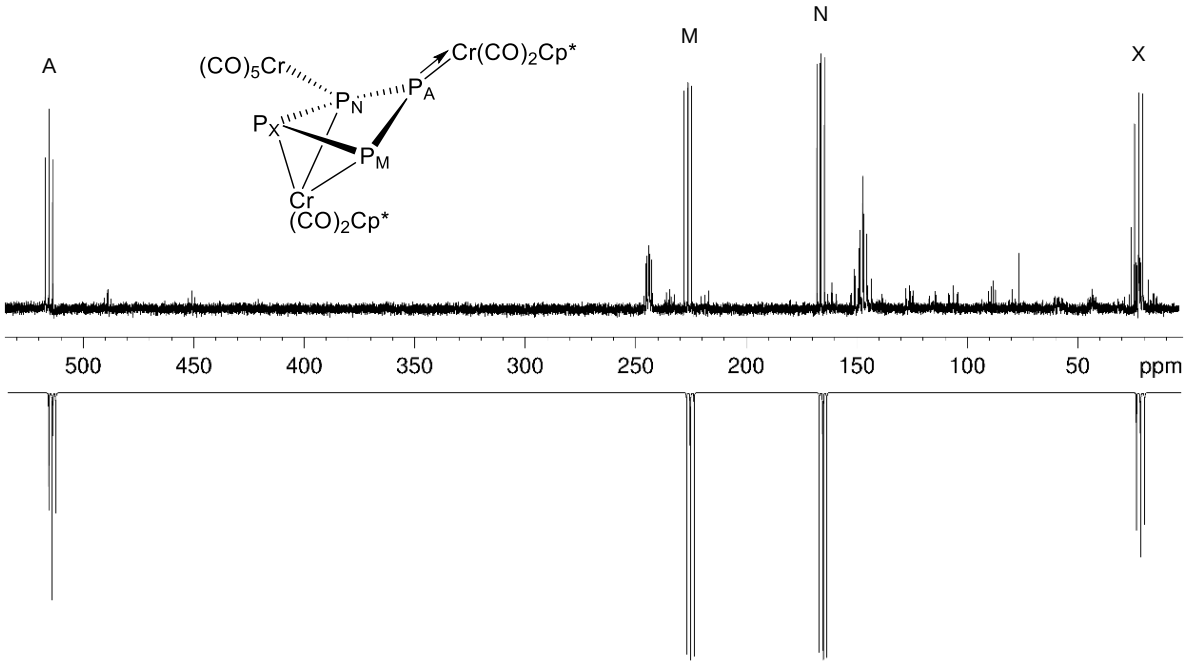

Figure S2. Experimental $^{31}P\{^1H\}$ NMR spectrum of the reaction of **1** with 1.0 eq. [Cr(CO)$_4$(nbd)] in CD_2Cl_2 (top) and simulated $^{31}P\{^1H\}$ NMR spectrum of **3a** (bottom).

[{Cp*Cr(CO)$_2$}$_2$(μ$_4$,η$^{3:1:1:1}$-P$_4$){Cr(CO)$_5$}$_2$] (4a)

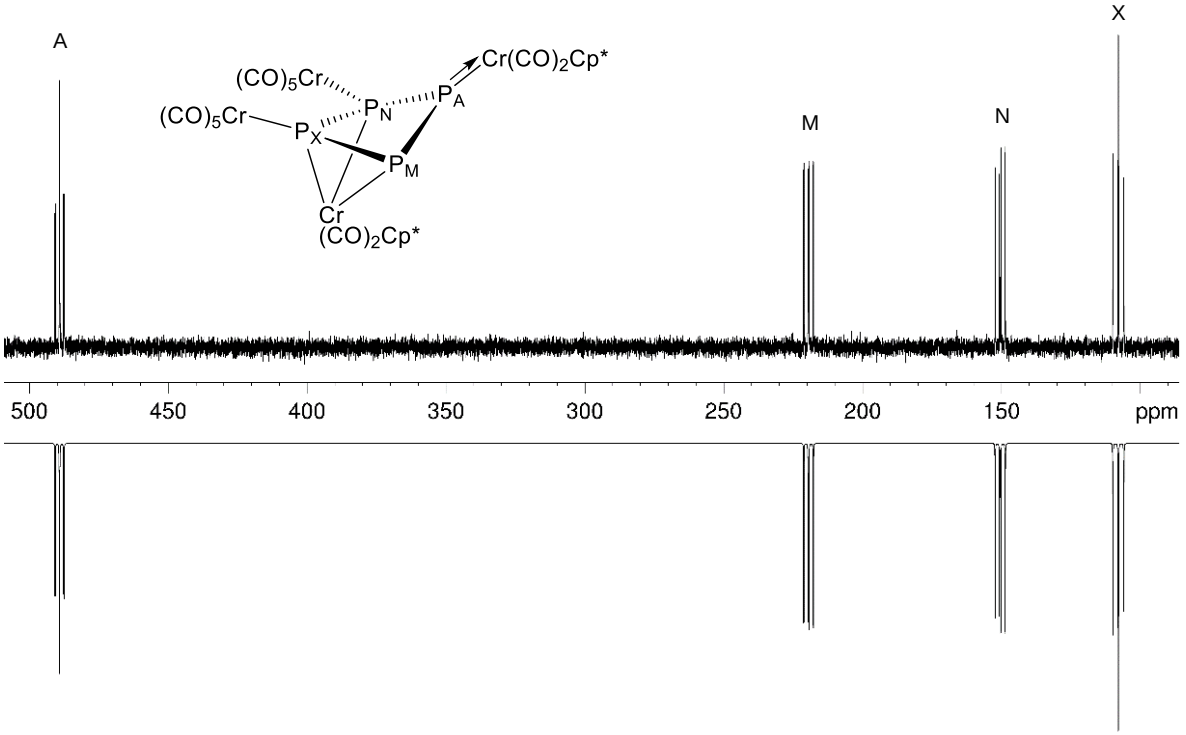

Figure S3. Experimental (top) and simulated (bottom) $^{31}P\{^1H\}$ NMR spectrum of **4a** in CD_2Cl_2.

[{Cp*Cr(CO)$_2$}$_2$(μ$_4$,η$^{3:1:1:1}$-P$_4$){Cr(CO)$_5$}$_2$] (4b)

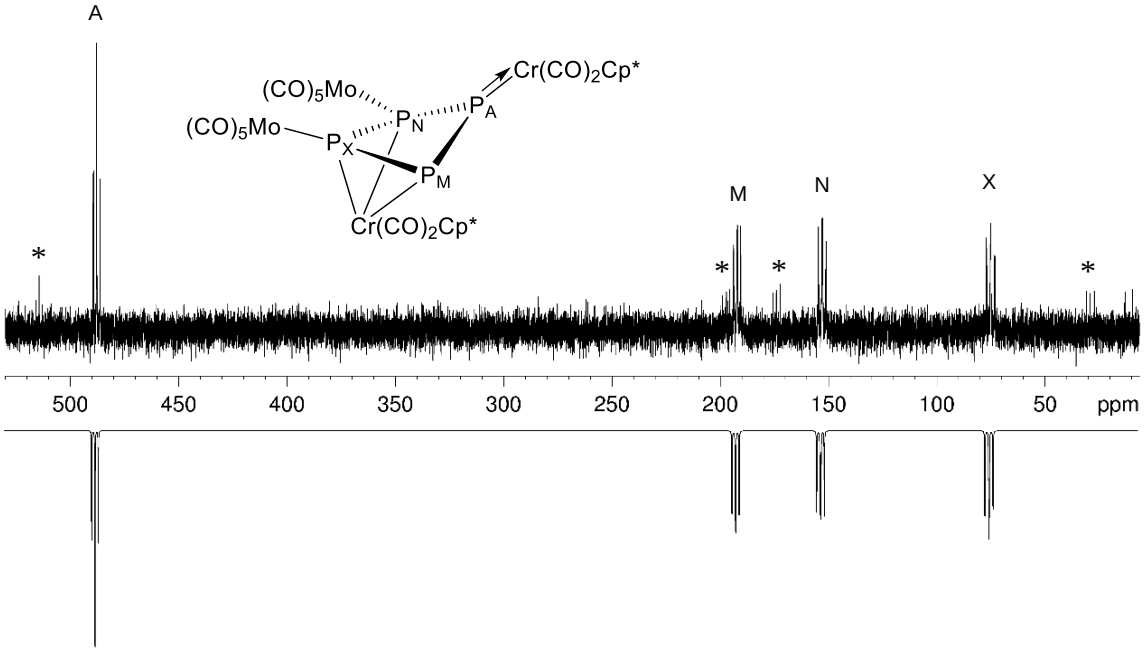

Figure S4. Experimental (top) and simulated (bottom) $^{31}P\{^1H\}$ NMR spectrum of **4b** in CD_2Cl_2 (Signals marked with * can be attributed to **3b** as a result of decomposition).

Table S2. Experimental and simulated values for the chemical shifts and coupling constants in the $^{31}P\{^1H\}$ NMR spectrum of **3a**, **4a** and **4b**.

	experimental values				simulated values[1]			
3a	δ_A	515.4 ppm	$^1J_{AM}$	251 Hz	δ_A	515.4 ppm	$^1J_{AM}$	249.3 Hz
	δ_M	226.3 ppm	$^1J_{AN}$	257 Hz	δ_M	226.3 ppm	$^1J_{AN}$	258.5 Hz
	δ_N	166.3 ppm	$^2J_{AX}$	-	δ_N	166.2 ppm	$^2J_{AX}$	6.8 Hz
	δ_X	22.3 ppm	$^2J_{MN}$	-	δ_X	22.3 ppm	$^2J_{MN}$	1.1 Hz
			$^1J_{MX}$	306 Hz			$^1J_{MX}$	306.2 Hz
			$^1J_{NX}$	290 Hz			$^1J_{NX}$	291.0 Hz
4a	δ_A	489.1 ppm	$^1J_{AM}$	254 Hz	δ_A	489.1 ppm	$^1J_{AM}$	256.0 Hz
	δ_M	219.5 ppm	$^1J_{AN}$	252 Hz	δ_M	219.6 ppm	$^1J_{AN}$	251.3 Hz
	δ_N	150.5 ppm	$^2J_{AX}$	28 Hz	δ_N	150.4 ppm	$^2J_{AX}$	26.9 Hz
	δ_X	107.9 ppm	$^2J_{MN}$	20 Hz	δ_X	108.0 ppm	$^2J_{MN}$	19.2 Hz
			$^1J_{MX}$	300 Hz			$^1J_{MX}$	230.0 Hz
			$^1J_{NX}$	330 Hz			$^1J_{NX}$	330.3 Hz
4b	δ_A	487.8 ppm	$^1J_{AM}$	-	δ_A	487.8 ppm	$^1J_{AM}$	247.3 Hz
	δ_M	192.2 ppm	$^1J_{AN}$	248 Hz	δ_M	192.1 ppm	$^1J_{AN}$	249.6 Hz
	δ_N	152.9 ppm	$^2J_{AX}$	24 Hz	δ_N	152.9 ppm	$^2J_{AX}$	22.6 Hz
	δ_X	75.2 ppm	$^2J_{MN}$	-	δ_X	75.2 ppm	$^2J_{MN}$	20.8 Hz
			$^1J_{MX}$	-			$^1J_{MX}$	286.9 Hz
			$^1J_{NX}$	-			$^1J_{NX}$	324.0 Hz

[1] based on an AMNX spin system with a C_1 symmetry.

Stepwise substitution from 3a to 4a

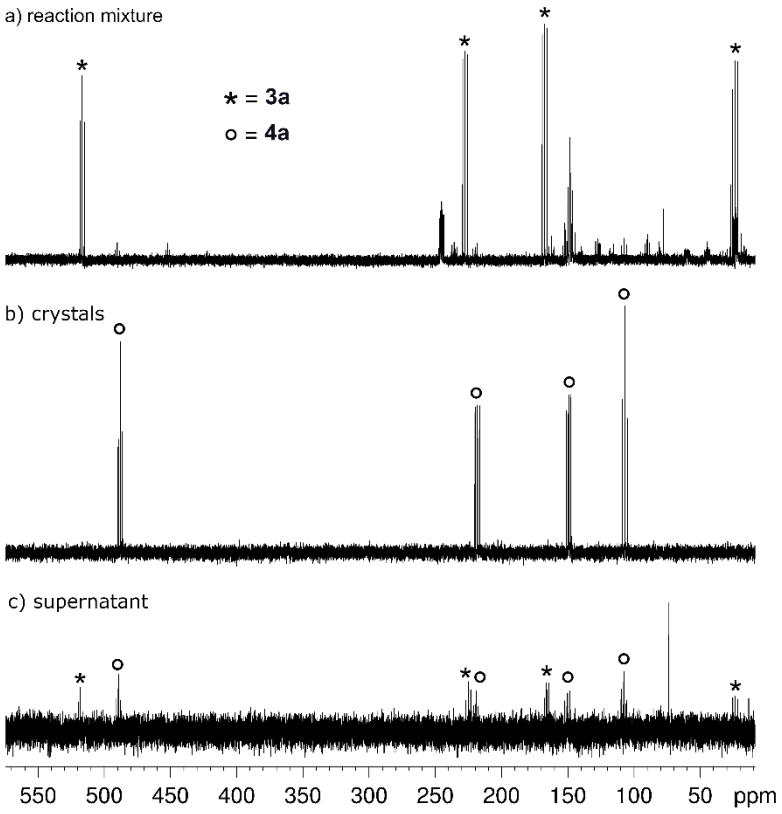

Figure S5: $^{31}P\{^{1}H\}$ NMR spectra of the reaction of **1** with 1.0 eq. $[Cr(CO)_4(nbd)]$: (a) reactions solution (b) dissolved crystals obtained from the reaction solution (c) supernatant of the obtained crystals.

Stepwise substitution from 3b to 4b

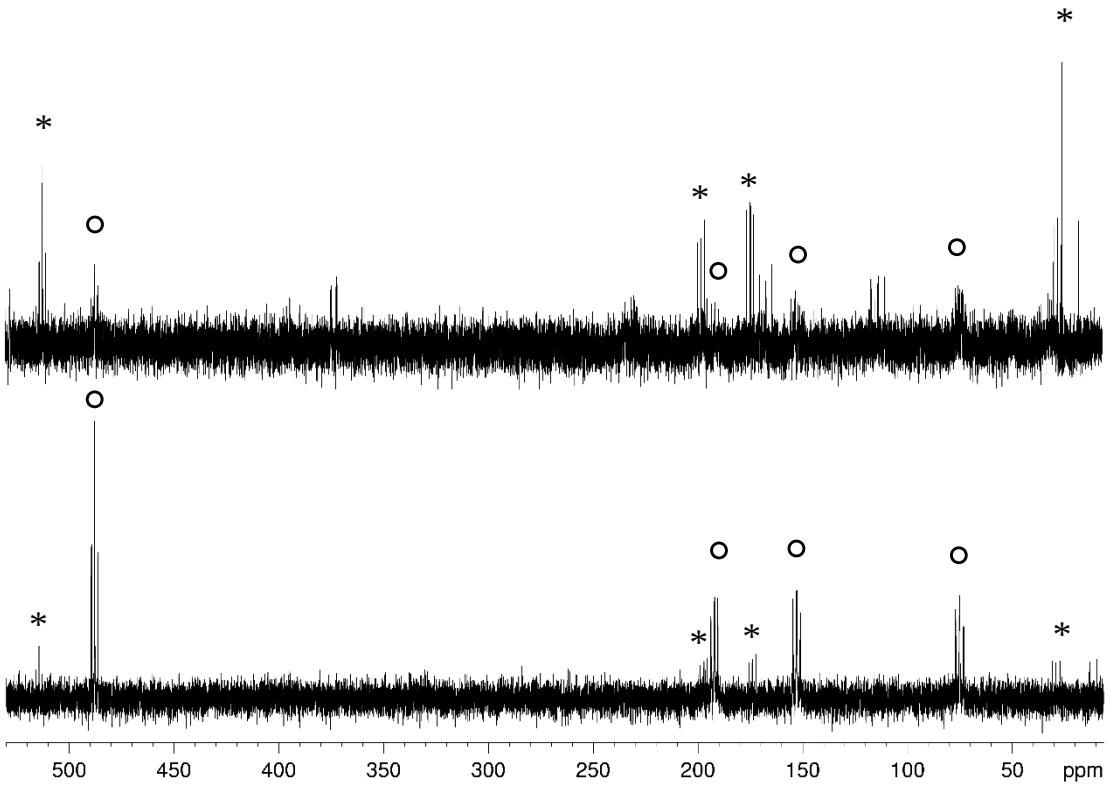

Figure S6. $^{31}P\{^{1}H\}$ NMR spectrum (in CD_2Cl_2) of the reaction solution (top) and the isolated crystals (bottom) from the reaction of **1** with 1.0 eq. $[Mo(CO)_4(nbd)]$. Signals marked with * can be attributed to **3b b**and signals marked with ° belong to **4b,** respectively.

As discussed for **3a** the mono-substituted **3b** is the main species in the reaction solution when reacting **1** with 1.0 eq. $[Mo(CO)_4(nbd)]$. When storing the solution at -28 °C during the crystallization process, a second substitution occurs giving **4b** as the exclusive crystallization product. However, if the crystals are dissolved in CD_2Cl_2 a small amount of **4b** decomposes to give **3b** as a side product.

2. DFT calculations of 4a

In order to elucidate the electronic structure of **4a**, DFT calculations at the BP86/def2-TZVP level were performed and the geometric parameters of the optimized geometry of **4a** are in good agreement with those determined by single crystal X-ray diffraction. According to the calculations, the short Cr1–P1 distance (labeling according to Figure 3) represents a double bond, as it is attributed a Wiberg Bond Index (WBI) of 1.43. Consequently, the additional coordination of electron density from the P1 lone pair towards Cr1 balancing the electron deficit caused by decarbonylation is confirmed. The WBIs of the Cr2–P bonds vary from 0.60 to 0.78, while the WBIs for the Cr3–P3 and Cr4–P4 bonds are both 0.71. The NPA charges (Natural Population Analysis) show a negative charge accumulation on the Cr atoms (Cr1: -0.91, Cr2: -1.15, Cr3: -1.61, Cr4: -1.61), while the P_4 unit is rather positively charged (P1: 0.34, P2: 0.10, P3: 0.31, P2: 0.41), which reflects the donating ability of the P_4 unit. Additionally, the calculated HOMO and HOMO-1 of **4a** represent the d-orbitals of the Cr1 atom, while the HOMO-2 and the HOMO-4 contain contributions from the Cr1–P1 multiple bond and the double bond nature of the Cr1–P1 bond is also shown by the localized molecular orbitals.

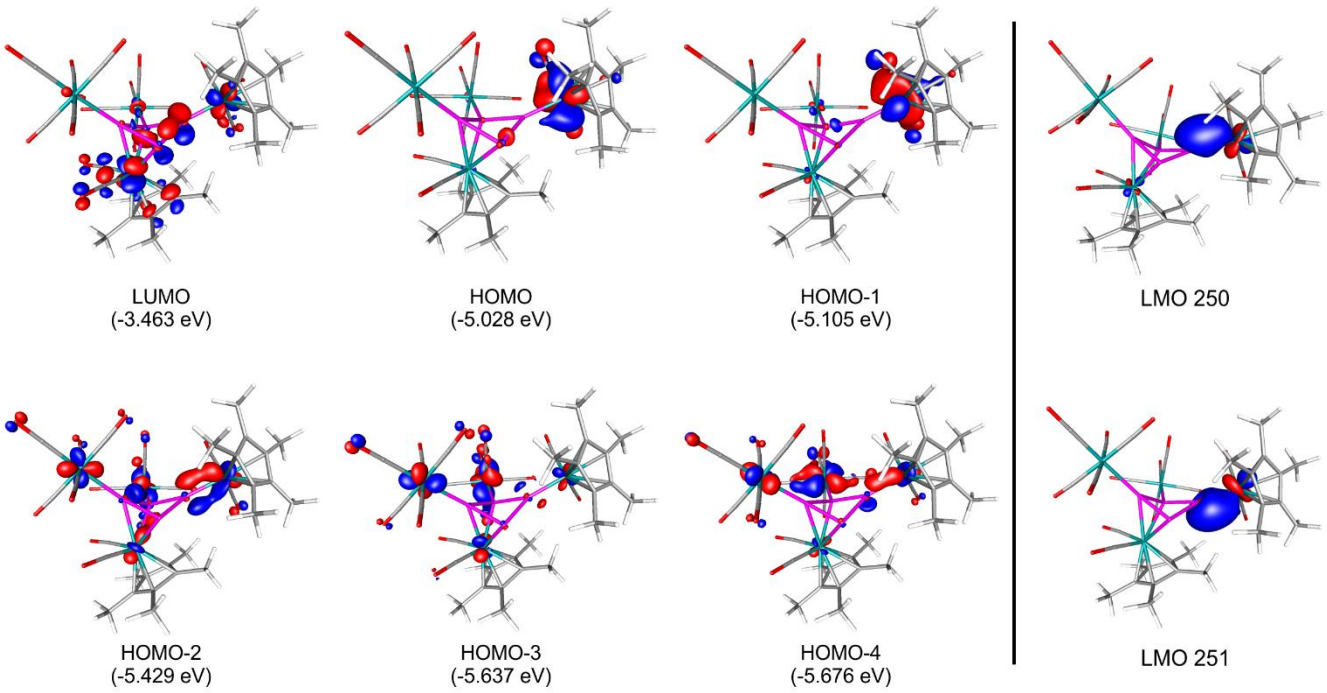

Figure S7. Left: Frontier molecular orbitals of **4a**, calculated at the BP86/def2-TZVP level of theory; right: Localized molecular orbitals representing the Cr1–P1 multiple bond in **4a**

3. Crystallographic section

The crystals were selected and mounted on a GV50 diffractometer equipped with a TitanS2 detector. All crystals were kept at T = 123(1) K during data collection. Data collection and reduction were performed with CrysAlisPro version 1.171.40.14a.[12] For all compounds a numerical absorption correction based on gaussian integration over a multifaceted crystal model and an empirical absorption correction using spherical harmonics, implemented in SCALE3 ABSPACK scaling algorithm was applied. Using Olex2,[13] all structures were solved by ShelXT[14] and a least-square refinement on F2 was carried out with ShelXL.[15] All non-hydrogen atoms were refined anisotropically. Hydrogen atoms at the carbon atoms were located in idealized positions and refined isotropically according to the riding model.

CCDC-2009816 (**2**), CCDC-2009704 (**3a**), CCDC-2009705 (**4a**), CCDC-2009706 (**4b**) and CCDC-2009707 (**5**), contain the supplementary crystallographic data for this paper. These data can be obtained free of charge at www.ccdc.cam.ac.uk/contents/retrieving.html (or from the Cambridge Crystallographic Data Centre, 12 Union Road, Cambridge CB2 1EZ, UK; Fax: +44-1223-336-033; e-mail: deposit@ccdc.com.ac.uk).

Table 3: overview of selected crystallographic parameters of the single crystal X-ray diffraction experiments performed for **2**, **3a**, **4a**, **4b** and **5**.

	2	**3a**	**4a**	**4b**	**5**
Formula	$C_{30}H_{30}Cr_2O_{10}P_4W$	$C_{30}H_{32}Cl_2Cr_3O_9P_4$	$C_{35}H_{32}Cl_2Cr_4O_{14}P_4$	$C_{35}H_{32}Cl_2Cr_2Mo_2O_{14}P_4$	$C_{12}H_{15}CrO_2P_3$
$D_{calc.}$ **/ g cm^{-3}**	1.790	1.583	1.639	1.721	1.582
m**/mm^{-1}**	12.906	10.458	11.028	11.297	9.816
Formula Weight	962.27	887.33	1079.38	1167.26	336.15
Colour	dark brown	dark orange	dark orange	dark green	light orange
Shape	block	plate	plate	plate	block
Size/mm^3	0.10×0.10×0.07	0.15×0.12×0.04	0.11×0.09×0.02	0.36×0.20×0.04	0.08×0.06×0.05
T**/K**	123.01(13)	123.01(10)	123.00(10)	123.0	123.01(10)
Crystal System	tetragonal	monoclinic	triclinic	triclinic	orthorhombic
Flack Parameter	-0.007(8)	-	-	-	-
Hooft Parameter	-0.008(6)	-	-	-	-
Space Group	$I\bar{4}$	$P2_1/c$	$P\bar{1}$	$P\bar{1}$	$Pnma$
a**/Å**	19.1084(4)	8.61978(12)	11.0293(5)	11.1540(3)	8.3549(2)
b**/Å**	19.1084(4)	21.5601(3)	11.2147(5)	11.2534(3)	12.7888(3)
c**/Å**	19.5531(6)	20.3044(2)	19.6309(7)	19.9843(5)	13.2096(2)
α**/°**	90	90	83.486(4)	83.065(2)	90
β**/°**	90	99.3350(13)	89.878(3)	89.507(2)	90
γ**/°**	90	90	65.220(5)	64.897(2)	90
V/Å^3	7139.4(4)	3723.47(9)	2187.57(18)	2252.35(10)	1411.44(6)
Z	8	4	2	2	4
Z'	1	1	1	1	0.5
Wavelength/Å	1.54184	1.54184	1.54184	1.54184	1.54184
Radiation type	Cu K_α	Cu K_α	Cu K_α	Cu K_α	Cu K_α
Q_{min}**/°**	3.234	4.101	4.376	4.375	4.813
Q_{max}**/°**	74.141	74.213	74.174	66.404	79.927
Measured Refl's.	18647	21477	18305	23984	7393
Ind't Refl's	6396	7429	8439	7857	1448
Refl's with I > 2(I)	5883	6622	6231	7480	1397
R_{int}	0.0577	0.0315	0.0584	0.0375	0.0245
Parameters	434	633	561	569	119
Restraints	0	520	18	66	0
Largest Peak	2.722	0.700	0.725	1.271	0.324
Deepest Hole	-1.883	-0.599	-0.627	-1.371	-0.370
GooF	1.082	1.026	1.018	1.036	1.083
wR_2 **(all data)**	0.1235	0.0760	0.1252	0.1235	0.0618
wR_2	0.1192	0.0728	0.1103	0.1215	0.0600
R_1 **(all data)**	0.0542	0.0353	0.0750	0.0449	0.0243
R_1	0.0483	0.0298	0.0484	0.0433	0.0230

$[\{Cp^*Cr(CO)_3\}_2(\mu_3,\eta^{1:1:1:1}\text{-}P_4)\{W(CO)_4\}]$ (2)

Compound **2** crystalizes in the form of dark brown blocks from a saturated solution in hexane/CH_2Cl_2 upon storage at -28°C. A suitable crystal with dimensions 0.10 × 0.10 × 0.07 mm^3 was selected and mounted on a GV50, TitanS2 diffractometer. The crystal was kept at a steady T = 123.01(13) K during data collection. The structure was solved with the ShelXT (Sheldrick, 2015) solution program using dual methods. The model was refined with ShelXL 2018/3 (Sheldrick, 2015) using full matrix least squares minimization on F^2. The asymmetric unit contains one molecule of **2**.

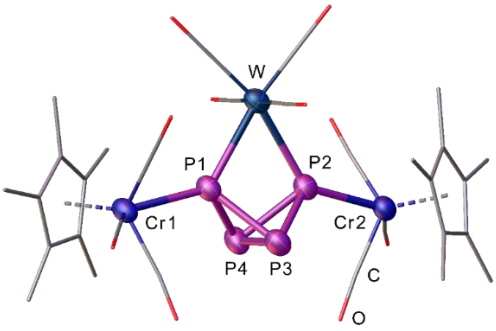

Figure S8. Molecular structure of **2** in the solid state; for clarity H atoms are omitted and the Cp* as well as CO ligands are drawn in the wire frame model; thermal ellipsoids drawn at 50% probability level.

Table S4: Selected bond lengths [Å] and angles [°] of **2**

d / Å		α / °	
Cr1–P1	2.449(4)	**P1–W–P2**	64.21(11)
Cr2–P2	2.445(4)	**P1–P3–P2**	76.21(17)
W–P1	2.583(4)	**P1–P4–P2**	76.51(17)
W–P2	2.582(3)	**P3–P1–P4**	59.49(17)
P1–P3	2.214(5)	**P3–P2–P4**	59.38(17)
P1–P4	2.224(5)	**P2-P4-P3**	60.86(17)
P2–P3	2.235(5)	**P1-P4-P3**	60.03(16)
P2–P4	2.210(5)	**P2-P3-P4**	59.75(16)
P1··P2	2.74(5)	**P1-P3-P4**	60.48(16)
P3–P4	2.202(6)		

SUPPORTING INFORMATION

[{Cp*Cr(CO)$_2$}$_2$(μ$_3$,η$^{3:1:1}$-P$_4$){Cr(CO)$_5$}] (3a)

Compound **3a** crystalizes in the form of dark orange plates from a reaction solution of **1** with 1.0 eq. [Cr(CO)$_4$(nbd)]. The reaction solution is stored at -78°C for one week and subsequently held at -28°C for three months. A suitable crystal with dimensions 0.15 × 0.12 × 0.04 mm^3 was selected and mounted on a GV50, TitanS2 diffractometer. The crystal was kept at a steady T = 123.01(10) K during data collection. The structure was solved with the ShelXT (Sheldrick, 2015) solution program using dual methods. The model was refined with ShelXL 2018/3 (Sheldrick, 2015) using full matrix least squares minimization on F^2.The asymmetric unit contains one molecule of Compound **3a** (displaying a highly disordered Cp* ligand) and one CH_2Cl_2 molecule.

[{Cp*Cr(CO)$_2$}$_2$(μ$_4$,η$^{3:1:1:1}$-P$_4$){Cr(CO)$_5$}$_2$] (4a)

Compound **4a** crystalizes in the form of dark orange plates from a saturated solution in CH_2Cl_2 upon storage at -28°C. A suitable crystal with dimensions 0.11 × 0.09 × 0.02 mm^3 was selected and mounted on a SuperNova, Single source at offset/far, Atlas diffractometer. The crystal was kept at a steady T = 123.00(10) K during data collection. The structure was solved with the ShelXT (Sheldrick, 2015) solution program using dual methods. The model was refined with ShelXL 2018/3 (Sheldrick, 2015) using full matrix least squares minimisation on F^2. The asymmetric unit contains one molecule of **4a** as well as one disordered solvent molecule.

[{Cp*Cr(CO)$_2$}$_2$(μ$_4$,η$^{3:1:1:1}$-P$_4$){Mo(CO)$_5$}$_2$] (4b)

Compound **4b** crystalizes in the form of dark green plates from a saturated solution in CH_2Cl_2/*n*-pentane upon storage at -28°C. A suitable crystal with dimensions 0.36 × 0.20 × 0.04 mm^3 was selected and mounted on a Xcalibur, AtlasS2, Gemini ultra diffractometer. The crystal was kept at a steady T = 123.0 K during data collection. The structure was solved with the ShelXT (Sheldrick, 2015) solution program using dual. The model was refined with ShelXL 2018/3 (Sheldrick, 2015) using full matrix least squares minimisation on F^2.The asymmetric unit contains one molecule of **4b** as well as one disordered solvent molecule.

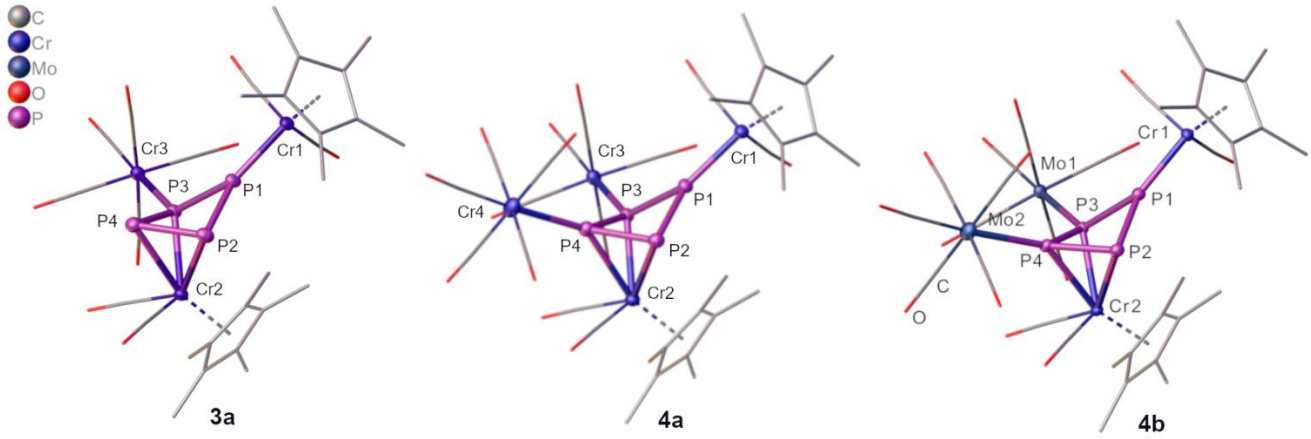

Figure S9. Molecular structure of Compound **3a, 4a** and **4b** in the solid state; for clarity H atoms and solvent molecules are omitted, Cp* and CO ligands are drawn in the wire frame model and only position of disordered Cp* ligand is displayed; thermal ellipsoids drawn at 50% probability level

Table S5: Selected bond lengths [Å] and angles [°] of **3a**, **4a** and **4b**.

		3a	4a	4b
d / Å	**Cr1–P1**	2.1258(6)	2.1129(11)	2.1169(11)
	Cr2–P2	2.4774(6)	2.4926(12)	2.4970(11)
	Cr2–P3	2.4451(5)	2.4778(11)	2.4726(11)
	Cr2–P4	2.4512(6)	2.4428(11)	2.4354(11)
	Cr3–P3 / Mo1-P3	2.3664(5)	2.3564(12)	2.5002(9)
	Cr4–P4 / Mo2-P4	-	2.3517(11)	2.4896(10)
	P1–P2	2.2181(7)	2.2265(13)	2.2259(13)
	P1–P3	1.1973(7)	2.2013(14)	2.1938(13)
	P3–P4	2.1705(7)	2.1583(12)	2.1560(13)
	P2–P4	2.1606(7)	2.1390(15)	2.1427(13)
α / °	**Cr1–P1–P2**	137.83(3)	138.98(6)	139.54(5)
	Cr1–P1–P3	139.04(3)	137.30(6)	136.42(5)
	P2–P1–P3	82.99(2)	83.72(5)	84.02(5)
	P1–P2–P4	86.79(2)	85.88(5)	85.66(5)
	P1–P3–P4	87.07(2)	86.04(5)	86.14(5)
	P2–P4–P3	84.98(3)	86.88(5)	86.96(5)
	$Plane_{P1–P2–P3}$ vs. $Plane_{P2–P3–P4}$	135.50(8)	135.92(6)	136.18(8)

$[Cp^*Cr(CO)_2(\eta^3\text{-}P_3)]$ (5)

Compound **5** crystalizes as light orange blocks from a saturated solution in *n*-hexane upon storage at -28°C. A suitable crystal with dimensions 0.08 × 0.06 × 0.05 mm^3 was selected and mounted on a GV50, TitanS2 diffractometer. The crystal was kept at a steady T = 123.01(10) K during data collection. The structure was solved with the ShelXT 2014/5 (Sheldrick, 2014) solution program. The model was refined with ShelXL 2018/3 (Sheldrick, 2015) using full matrix least squares minimisation on F^2.The asymmetric unit contains half a molecule of **5.**

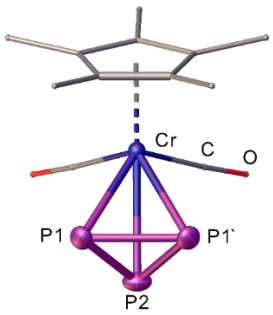

Figure S10. Molecular structure of **5** in the solid state; for reasons of clarity H atoms are omitted and the Cp* as well as CO ligands are drawn in the wire frame model; thermal ellipsoids drawn at 50% probability level.

Table S6: Selected bond lengths [d/Å] and angles [α/°] of **5**

d / Å		α / °	
Cr–P1	2.4773(5)	**P1–P1`–P2**	60.646(15)
Cr–P1`	2.4773(5)	**P1–P2–P1`**	58.71(3)
Cr–P2	2.5406(7)		
P1–P2	2.1205(7)		
P1–P1`	2.0790(8)		

References

[1] a) R. B. King, *J. Organomet. Chem.* **1967**, *8*, 139-148; b) P. Leoni, A. Landi, M. Pasquali, *J. Organomet. Chem.* **1987**, *321*, 365-369; c) T. J. Jaeger, M. C. Baird, *Organometallics* **1988**, *7*, 2074-2076; d) C. Schwarzmaier, A. Y. Timoshkin, G. Balázs, M. Scheer, *Angew. Chem. Int. Ed.* **2014**, *53*, 9077-9081.

[2] R. B. King, A. Frozalia, *Inorg. Chem.* **1966**, *5*, 1837.

[3] TopSpin 3.0, Bruker BioSpin GmbH

[4] R. C. Clark, J. S. Reid, *Acta Cryst.* **1995**, *A51*, 887-897.

[5] CrysAlisPRO, Oxford Diffraction /Agilent Technologies UK Ltd, Yarnton, England.

[6] a) O. V. Dolomanov, L. J. Bourhis, R. J. Gildea, L. A. K. Howard, H. Puschmann, *J. Appl. Cryst.* **2009**, 42, 339-341; b) G. Sheldrick, *Acta Cryst.* **2008**, A*64*, 112-122.

[7] a) F. Furche, R. Ahlrichs, C. Hättig, W. Klopper, M. Sierka, F. Weigend, *WIREs Comput. Mol. Sci.* **2014**, *4*, 91-100; b) R. Ahlrichs, M. Bär, M. Häser, H. Horn, C. Kölmel, *Chem. Phys. Lett.* **1989**, *162*, 165–169; c) O. Treutler, R. Ahlrichs, *J. Chem. Phys.* **1995**, *102*, 346–354.

[8] a) K. Eichkorn, O. Treutler, H. Oehm, M. Häser, R. Ahlrichs, *Chem. Phys. Lett.* **1995**, *242*, 652–660; b) K. Eichkorn, F. Weigend, O. Treutler, R. Ahlrichs, *Theor. Chem. Acc.* **1997**, *97*, 119.

[9] a) P. A. M. Dirac *Proc. Royal Soc. A*, **1929**, *123*, 714–733.; b) J. C. Slater *Phys. Rev.*, **1951**, *81*, 385–390; c) S. Vosko; L. Wilk; M. Nusair, *Can. J. Phys.*, **1980**, *58*, 1200–1211; d) A. D. Becke *Phys. Rev. A*, **1988**, *38*, 3098–3100; e) J. P. Perdew. *Phys. Rev. B*, **1986**, *33*, 8822–8824.

[10] a) A. Schäfer, C. Huber, R. Ahlrichs, *J. Chem. Phys.* **1994**, *100*, 5829; b) K. Eichkorn, F. Weigend, O. Treutler, R. Ahlrichs, *Theor. Chem. Acc.* **1997**, *97*, 119; c) F. Weigend, R. Ahlrichs, *Phys. Chem. Chem. Phys.* **2005**, *7*, 3297; d) F. Weigend, *Phys. Chem. Chem. Phys.* **2006**, *8*, 1057.

[11] M. Sierka, A. Hogekamp, R. Ahlrichs, *J. Chem. Phys.* **2003**, *118*, 9136.

[12] CrysAlisPro Software System, Rigaku Oxford Diffraction, (**2018**).

[13] a) L. J. Bourhis, O. V. Dolomanov, R. J. Gildea, J. A. K. Howard, H. Puschmann, The Anatomy of a Comprehensive Constrained, Restrained, Refinement Program for the Modern Computing Environment - **Olex2** Disected, *Acta Cryst. A* **2015**, A71, 59–71; b) O. V. Dolomanov, L. J. Bourhis, R. J. Gildea, J. A. K. Howard, H. Puschmann, Olex2: A complete structure solution, refinement and analysis program, *J. Appl. Cryst.* **2009**, 42, 339–341.

[14] G. M. Sheldrick, ShelXT-Integrated space-group and crystal-structure determination, *Acta Cryst.* **2015**, A71, 3–8.

[15] G. M. Sheldrick, Crystal structure refinement with ShelXL, *Acta Cryst.* **2015**, C71, 3–8.